Preparation, Structures, and Electrochemistry of a New Polyoxometalate-Based Organic/Inorganic Film on Carbon Surfaces

Zhiyong Tang, Shaoqin Liu, Erkang Wang,* and Shaojun Dong*

Laboratory of Electroanalytical Chemistry, Changchun Institute of Applied Chemistry, Chinese Academy of Sciences, Changchun 130022, P. R. China

Enbo Wang

Department of Chemistry, The Northeast Normal University, Changchun 130021, P. R. China

Received October 13, 1999. In Final Form: April 3, 2000

The preparation, structure, and electrochemical and electrocatalytical properties of a new polyoxometalate-based organic/inorganic film, composed of cetyl pyridinum 11-molybdovanadoarsenate (CPMVA) molecules, have been studied. Cyclic potential scanning in acetone solution led to a stable CPMVA film formed on a highly oriented pyrolytic graphite (HOPG) surface. X-ray photoelectron spectroscopy, scanning tunneling microscopy, and cyclic voltammetry were used for characterizing the structure and properties of the CPMVA film. These studies indicated that self-aggregated clusters were formed on a freshly cleaved HOPG surface, while a self-organized monolayer was formed on the precathodized HOPG electrode. The CPMVA film exhibited reversible redox kinetics both in acidic aqueous and in acetone solution, which showed that it could be used as a catalyst even in organic phase. The CPMVA film remained stable even at pH >7.0, and the pH dependence of the film was much smaller than that of its inorganic film ($H_4AsMo_{11}VO_{40}$) in aqueous solution. The CPMVA film showed strong electrocatalysis on the reduction of bromate, and the catalytic currents were proportional to the square of the concentration of bromate. The new kind of polyoxometalate with good stability may have extensive promise in catalysis.

Introduction

Polyoxometalates have won particular attention for their applications in many fields of science such as medicine,[1] biology,[2] catalysis,[3] and materials[4−6] owing to their chemical, structural, and electronic versatility. One of the most important properties of these metal oxide clusters is the capability for reversible multivalence reduction, forming mixed-valence species. The property makes them very useful in the preparation of modified electrodes[7−9] and brings about favorable catalytic properties with regard to several challenging electrochemical processes such as the reduction of nitrite.[10] So, how to design new kinds of polyoxometalates and successfully immobilize them on electrode surfaces, while maintaining and/or enhancing their beneficial properties, is fascinating to chemists. Multilayer formation on electrodes has recently been reported to improve the properties of polyoxometalates through layer-by-layer self-assembly (LBL) or the Langmuir−Blodgett (LB) method.[11] These techniques are shown to be a rapid and easy way to obtain ordered molecular assemblies with precise control of layer composition and thickness.

The present report focuses mainly on the design and properties of a new polyoxometalate-based material. Primarily, we hope that the new material can easily be obtained; its catalytic and electrocatalytic activity can be retained and even enhanced when it is immobilized on

* To whom correspondence should be addressed.

(1) Bussereau, F.; Picard, M.; Malik, C.; Teze, A.; Blancou, J. *Ann. Inst. Pasteur/Virol.* **1988**, *32*, 33.

(2) Ono, K.; Nakane, H.; Barre-Sinoussi, F.; Chermann, C. *Nucleic Acids Res. Symp. Ser.* **1984**, *15*, 169.

(3) (a) Misono, M. *Catal. Rev. Sci. Eng.* **1987**, *29*, 269. (b) Haeberle, T.; Emig. G. *Chem. Eng. Technol.* **1988**, 392. (c) Watzenberger A.; Emig, G.; Lynch, D. T. *J. Catal.* **1990**, *124*, 247.

(4) (a) Pope, M. T.; Muller, A. *Angrew. Chem., Int. Ed. Engl.* **1991**, *30*, 34. (b) Pope, M. T. *Heteropoly and Isopoly Polyoxometalates*; Springer-Verlag: Berlin, 1983. (c) Pope, M. T.; Muller, A. *Polyoxometalates: From Platonic Solids to Antiretroviral Activity*; Kluwer: Dordrecht, Netherlands, 1994.

(5) Shimidzu, T.; Ohtami, A.; Aiba, M.; Honda, K. *J. Chem. Soc., Faraday Trans.* **1988**, *84*, 3941.

(6) Ouahab, L. *Chem. Mater.* **1997**, *9*, 1909.

(7) (a) Dong, S.; Wang, B. *Electrochim. Acta* **1992**, *37*, 11. (b) Wang, B.; Dong, S. *Electrochim. Acta* **1992**, *37*, 1859. (c) Wang, B.; Dong, S. *J. Electroanal. Chem.* **1992**, *328*, 245. (d) Dong, S.; Song, F.; Wang, B.; Liu, B. *Electroanalysis* **1992**, *4*, 643. (e) Dong, S.; B. Wang, F. Song, *Chem. Lett.* **1992**, *215*, 414. (f) Dong, S.; Jin, Z. *Chin. Chim. Acta* **1989**, *47*, 922. (g) Dong, S.; Jin, W. *J. Electroanal. Chem.* **1993**, *354*, 87. (h) Dong, S.; Liu, M. *Electrochim. Acta* **1994**, *39*, 947.

(8) (a) Bidan, G.; Genies, E. M.; Lapkowski, M. *J. Electroanal. Chem.* **1988**, *251*, 297. (b) Bidan, G.; Genies, E. M.; Lapkowski, M. *Synth. Met.* **1989**, *31*, 327. (c) Lapkowski, M.; Bidan, G.; Fournier, M. *Synth. Met.* **1991**, *41*, 407. (d) Bidan, G.; Lapkowski, M.; Travers, J. P. *Synth. Met.* **1989**, *28*, 113. (e) Fabre, B.; Bidan, G.; Lapkowski, M. *J. Chem. Soc., Chem. Commun.* **1994**, 1509.

(9) (a) Keita, B.; Belhouari, A.; Nadjo, L.; Contant, R. *J. Electroanal. Chem.* **1995**, *381*, 243. (b) Keita, B.; Nadjo, L. *J. Electroanal. Chem.* **1988**, *255*, 303. (c) Keita, B.; Essaadi, K.; Nadjo, L. *J. Electroanal. Chem.* **1989**, *259*, 127. (d) Keita, B.; Mahmoud, A.; Nadjo, L. *J. Electroanal. Chem.* **1995**, *386*, 245. (e) Sung, H.; So, H.; Paik, W. *Electrochim. Acta* **1994**, *39*, 645. (f) Keita, B.; Nadjo, L. *J. Electroanal. Chem.* **1987**, *227*, 1019. (g) Keita, B.; Nadjo, L. *J. Electroanal. Chem.* **1987**, *230*, 85. (h) Keita, B.; Nadjo, L. *J. Electroanal. Chem.* **1988**, *243*, 87. (i) Keita, B.; Nadjo, L. *J. Electroanal. Chem.* **1988**, *247*, 157. (j) Keita, B.; Nadjo, L. *J. Electroanal. Chem.* **1993**, *354*, 295.

(10) (a) Toth, J. E.; Anson, F. C. *J. Am. Chem. Soc.* **1989**, *111*, 2444. (b) Dong, S.; Liu, M. *J. Electroanal. Chem.* **1994**, *372*, 95. (c) Fabre, B.; Bidan, G.; Lapkowski, M. *J. Chem. Soc., Chem. Commun.* 1994, 1509. (d) Keita, B.; Nadjo, L. *Mater. Chem. Phys.* **1989**, *22*, 77.

(11) (a) Moriguchi, I.; Hanai, K.; Hoshikuma, A.; Teraoka, Y.; Kagawa, S. *Chem. Lett.* 1994, 691. (b) Ingersoll, D.; Kulesza, J. P.; Faulkler, L. R. *J. Electrochem. Soc.* **1994**, *141*, 140. (c) Kuhn, A.; Anson, F. C. *Langmuir* **1996**, *12*, 5481. (d) Moriguchi, I.; Fendler, J. *Chem. Mater.* **1998**, *10*, 2205. (e) Clemente-Leon, M.; Beatrice, A.; Mingotaud, C.; Gomez-Garcia, C. J.; Coronado, E.; Delhaes, P. *Langmuir* **1997**, *13*, 2340. (f) Clemente-Leon, M.; Mingotaud, C.; Agricole, B.; Gomez-Garcia, C. J.; Coronado, E.; Delhaes, P. *Angrew. Chem., Int. Ed. Engl.* **1997**, *36*, 1114.

10.1021/la991348e CCC: $19.00
Published on Web 05/27/2000

Scheme 1. View of the Structure of $AsMo_{11}VO_{40}^{4-}$ Anion (A) and Cetyl Pyridinum (B)

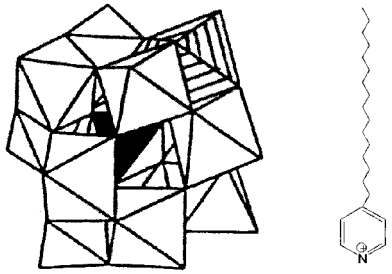

(a) $AsMo_{11}VO_{40}^{4-}$ (b) cetylpyridium

substrate surfaces. Second, the new material is anticipated to be used in a larger pH range, instead of only in acid solution. Third, the new material exhibits good catalytical activity even in organic solution. The amphiphilic molecules and organic−inorganic composite have been widely used as chemical sensor, modified electrode, or molecular electronic devices.[12] But scarce research, designing polyoxometalate-based amphiphilic molecules, has been done to enhance properties of polyoxometalates in catalysis. Indeed the Coulombic interaction between the positively charged lipid and the negatively charged polyoxometalate can stabilize the structure of polyoxometalates and enhance their properties in catalysis.

This paper describes that a new organic−inorganic film, cetyl pyridinum 11-molybdovanadoarsenate, was built on carbon surfaces. HOPG, an ideal carbon single-crystal material used to simplify the structural complexity, was chosen as the carbon substrate in the experiments. X-ray photoelectron spectroscopy (XPS), scanning tunneling microscopy (STM), and electrochemistry were used to characterize the structure and stability of the film. The electrochemical behavior of this organic−inorganic film was discussed, and electrocatalytical reduction of BrO_3^- with the CPMVA film was demonstrated in detail.

Experimental Section

Chemicals. $(C_{21}H_{38}N)_4AsMo_{11}VO_{40}$ (the molecular structure is shown in Scheme 1) was synthesized as follows: a stoichiometric ethanol solution of cetyl pyridium bromide was added to a solution of $H_4AsMo_{11}VO_{40}\cdot 18H_2O$ (pH 1.0). After vigorous stirring for 30 min, a yellow precipitate formed and was collected on a medium glass frit. After being washed by water, ethanol, and ether, the solid was dried under vacuum. Elemental analysis calculated (found): Mo, 32.8 (32.8); V, 1.58 (1.61); As, 2.33 (2.40); C, 31.37 (31.20); H, 5.23 (5.13); N, 1.74 (1.78). Infrared spectrum (cm^{-1}): 761.4, 840.4, 880.9, 941.4, 1373, 1482.1, 1451, and 1627.6. ^{51}V NMR: one resonance for V atom at $\delta = 73.180$.

All other reagents were of analytical grade and were used without further purification. Pure water was obtained by passing it through a Millipore Q water purification apparatus.

Electrochemical Experiments. Electrochemical experiments were carried out on CH Instruments (model 600 Voltammetric Analyzer). A three-electrode system was employed with an Ag|AgCl (saturated with KCl) or $Ag|Ag^+$ (0.1 M $AgNO_3$ in acetonitrite) electrode as reference electrode, a Pt electrode as counter electrode, and a highly oriented pyrolytic graphite (HOPG) electrode as working electrode.

Electrode Pretreatment Methods. The HOPG electrodes were then treated by three different methods and designated accordingly as follows: (i) clear surfaces of HOPG were obtained by peeling off the outer layers of the graphite; (ii) preanodized HOPG electrodes were polarized for 120 s at 1.5 V; (iii) precathodized HOPG electrodes were polarized for 120 s at −1.5 V.

A 0.5 M H_2SO_4 solution was used as the electrolyte for electrodes pretreatment.

XPS. The XPS spectra were recorded with an ESCALAB MK II Spectrometer. Mg Kα radiation was used as the X-ray source (1252.6 eV) with a pass energy of 50 eV. The pressure inside the analyzer was maintained at 10^{-9} Torr.

STM. The STM images were obtained in air with a Topometrix (Santa Clara, CA) TMX 2000 and a Digital (Santa Barbara, CA) Nano IIIA instrument. Electrochemically etched Pt/Ir tips were used.[13] Scanning was in the constant-current mode at a positive sample bias of 50−100 mV and tunneling current of 1−2 nA.

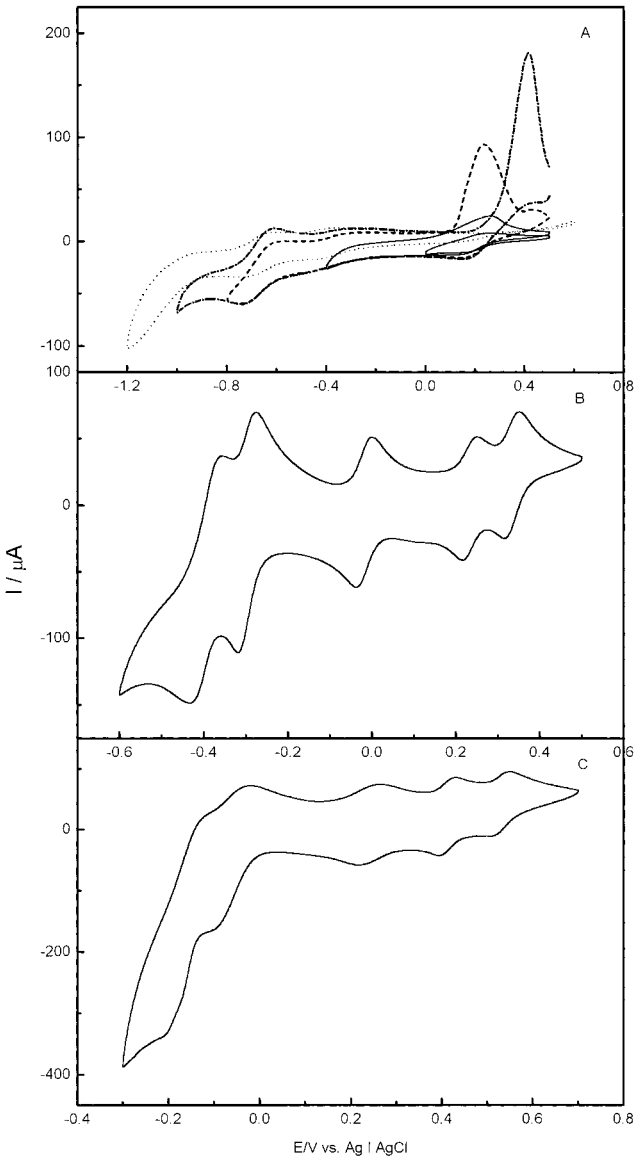

Figure 1. Cyclic voltammograms of 1 mM CPMVA in acetone + 0.1 M $LiClO_4$ solution at the HOPG electrode (A), after addition of 0.1 M $HClO_4$ (B), and 2 mM $H_4AsMo_{11}VO_{40}$ in 0.5 M H_2SO_4 (C). Scan rate: 100 mV s^{-1}.

Results and Discussions

1. Electrochemical Behavior of CPMVA in Acetone. CPMVA is soluble in acetone but not in aqueous solution. So electrochemical experiments of CPMVA were performed in acetone. Figure 1A shows cyclic voltammograms of 1 mM CPMVA in acetone containing 0.1 M

(12) Ulman, A. *Introduction to ultrathin organic films*, 1st ed.; Academic Press: Boston, MA, 1991.

(13) Zhang, B.; Wang, E. *Electrochim. Acta* **1994**, *39*, 103.

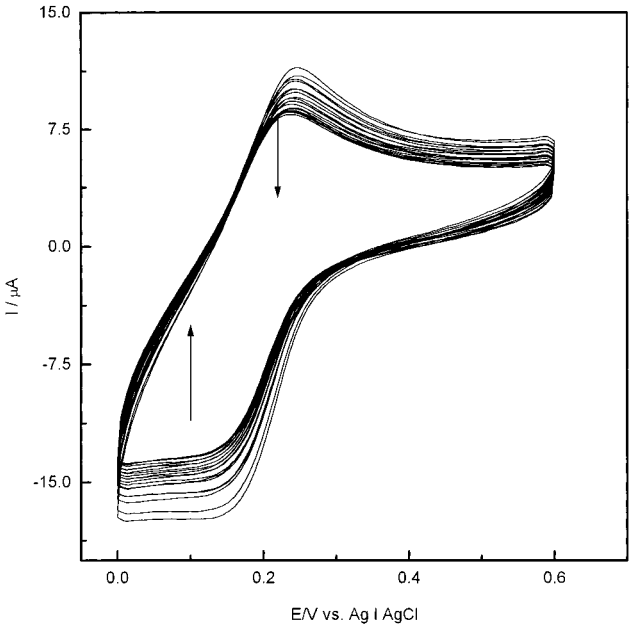

Figure 2. Cyclic voltammograms of l mM CPMVA in 0.1 M $LiClO_4$ + acetone solution at the freshly cleaved HOPG electrode. Scan rate: 100 mV s^{-1}.

$LiClO_4$. In the potential range of 0.50 and 0.0 V, CPMVA exhibits a quasi-reversible one-electron redox wave with the midpoint potential $E_{1/2} = (E_{pa} + E_{pc})/2$ of 0.20 V, where E_{pa} and E_{pc} are the cathodic and anodic peak potentials, respectively. Each current depends on the square root of the scan rate (10−500 mV s^{-1}), indicating that the electrode process is diffusion-controlled. However, when the lower limit of potential scans gets more negative, the cathodic peak remains unchanged, and the reoxidation process of CPMVA becomes very complicated. So in this paper, the film-formation potential is controlled in the range of only one wave occurring.

For all the Keggin anions, the addition of acid to the acetone system causes the one-electron waves to change into two-electron waves in a complex manner. Figure 1B shows the cyclic voltammogram of 1 mM CPMVA in acetone containing 0.1 M $LiClO_4$ with 0.1 M $HClO_4$. The cyclic voltammogram consists of five well-defined waves with $E_{1/2}$ of 0.33 V (I), 0.24 V (II), −0.02 V (III), −0.30 V (IV), and −0.40 V (V), and the $\Delta E_p = (E_{pa} - E_{pc})$ of 32, 35, 35, 73, and 62 mV, respectively. The voltammogram of CPMVA is similar to that of $H_4AsMo_{11}VO_{40}$ in acidic aqueous solution (Figure 1C). Coulombic studies show that these five reduction waves correspond to three two-electron-transfer followed by two four-electron-transfer processes. With further addition of acid, the peak potentials shift to more positive.

2. Preparation of the CPMVA Film. The CPMVA film on HOPG electrode is obtained by immersing HOPG electrode in 1 mM CPMVA of acetone solution containing 0.1 M $LiClO_4$ under cyclic scanning between 0.5 and 0.0 V at 100 mV s^{-1}. Figure 2 shows the cyclic voltammograms obtained during film growth on a freshly cleaved HOPG electrode. Only one quasi-reversible redox couple appears in the potential range of 0.60 and 0.0 V, and the peak current decreases continuously with increasing cycling time. Similar phenomenon of peak current decrease is observed at the precathodized HOPG electrode in 1 mM CPMVA of acetone solution. Although the structure of CPMVA film is different on the preanodized and precathodized substrates (discussed in the next section), on both preanodized and precathodized surfaces the direct part of the CPMVA film facing the acetone solution containing CPMVA molecules is the hydrophobic alkyl chains of the CPMVA film (as shown in Figure 4). The alkyl chains of the CPMVA film on both electrode surfaces limit access of solution-phase molecules to the electrode surface, so the peak current of CPMVA molecules in acetone solution decreases with the CPMVA film formation. On the contrary, when the precathodized HOPG electrode is immersed in 1 mM $H_4AsMo_{11}VO_{40}$ of acidic aqueous solution, the peak currents increase continuously with increasing cycling time. After 50 cycles of potential scanning, the peak current becomes stable and the CPMVA film is formed on the HOPG electrode surface. The electrode is removed from the acetone and rinsed thoroughly with a 0.5 M H_2SO_4 electrolyte solution.

3. Structures of the CPMVA Film. *XPS.* The presence of the CPMVA film on the HOPG electrode surface can be confirmed by XPS data. The relative molar ratios of N_{1s}, V_{2p}, and Mo_{3d} level XPS spectra of the CPMVA film (prepared as in section 2.3) are presented in Table 1 (assuming the molar quantity of V_{2p} % as 1).

The expected signals of N(1s) found at 401.2 eV are attributed to the pyridinum N^+ moiety. The two deconvoluted peaks at 235.8 and 232.6 eV are consistent with spin−orbit splitting of the Mo 3d level of Mo in the oxidation state +6.[14]

An elemental ratio of nitrogen to molybdenum is employed to estimate the molar amount of cetyl pyridinum cation to $AsMo_{11}VO_{40}^{4-}$ anion. The N/Mo atomic ratio is evaluated from the corresponding XPS intensities, window width, and photoionization cross sections for Mg Kα. According to the values in Table 1, the ratio of cetyl pyridinum nitrogen versus molybdenum atom is $N^+/Mo^{6+} = 4:(11 \pm 0.2)$ for the CPMVA film adsorbed on both freshly cleaved and precathodized electrode surfaces. It is consistent with the molecular composition of CPMVA in which four cetyl pyridinum cations are adsorbed on one $AsMo_{11}VO_{40}^{4-}$ anion. The XPS results also demonstrate that there are no cetyl pyridinum cations to be replaced by protons in the solution during CPMVA film formation. We also find that the ratio of N^+ versus Mo^{6+} remains unchanged even after immersing in 0.5 M H_2SO_4 for 3 h or cycling the potential between 0.70 and 0.0 V at 100 mV s^{-1} in 0.5 M H_2SO_4 for 1 h. It shows that the cetyl pyridinum ligands can steadily be adsorbed on the $AsMo_{11}VO_{40}^{4-}$ anion surface and proton exchange does not occur in acidic solution.

STM. STM offers an opportunity to characterize microscopic arrangement of polyoxometalates on a substrate.[15] Figure 3A shows a typical macroscale STM image of the CPMVA film adsorbed on a freshly cleaved HOPG surface. The white spots and irregular islands, with the range from nanometers to several hundred nanometers, represent the aggregated CPMVA molecules, which are never observed on a bare HOPG substrate. From the cross section, one can see that the height of CPMVA aggregates can reach about 16 nm. High-resolution and reproducible STM images of CPMVA molecules could not be obtained.

(14) (a) Briggs, D.; Seach, M. P. *Practical Surface Analysis by Auger and X-ray Photoelectron Spectroscopy*; Wiley: New York, 1983. (b) *Handbook of X-ray Photoelectron Spectroscopy*; Perkin-Elmer: Eden Prairie, MN, 1978. (c) Grunert, W.; Stakheev, A. Y.; Feldhaus, R.; Anders, K.; Shpire, E. S.; Minachev, K. M. *J. Phys. Chem.* **1991**, *95*, 1323.

(15) (a) Keita, B.; Nadjo, L.; Kjoller, K. *Surf. Sci.* **1991**, *256*, L613. (b) Watson, B. A.; Barteau, M. A.; Haggerty, L.; Lenhoff, A. M.; Weber, R. S. *Langmuir* **1992**, *8*, 1145. (c) Keita, B.; Chauveau, F.; Theobald, F.; Belanger, D.; Nadjo, L. *Surf. Sci.* **1992**, *264*, 271. (d) Zhang, B.; Wang, E. *J. Electroanal. Chem.* **1995**, *388*, 207. (e) Song, I. K.; Kaba, M. S.; Coulston, G.; Kourtakis, K.; Barteau, M. A. *Chem. Mater.* **1996**, *8*, 2352. (f) Song, I. K.; Kaba, M. S.; Barteau, M. A. *J. Phys. Chem.* **1996**, *100*, 17528.

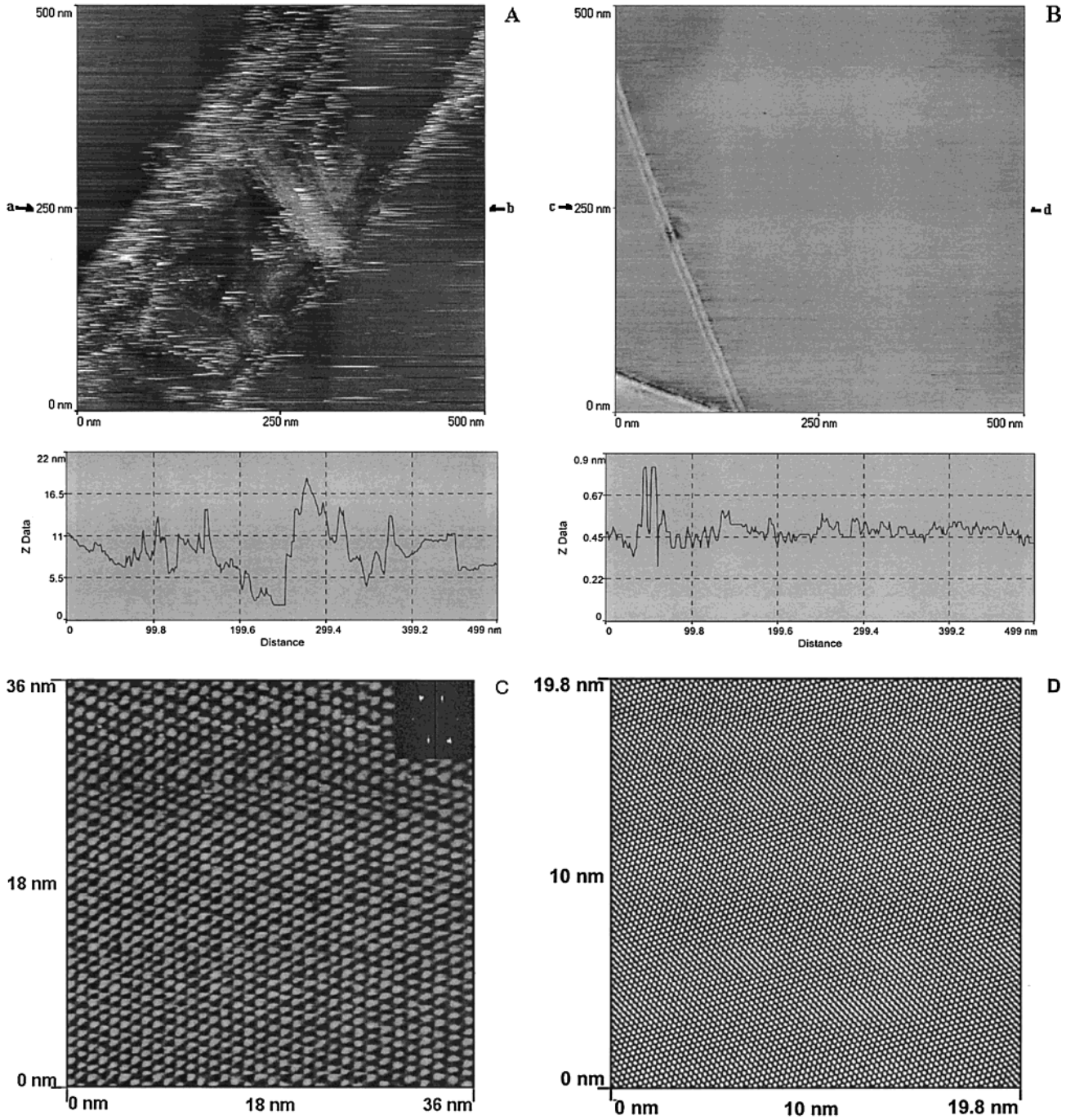

Figure 3. (A) STM images of CPMVA film adsorbed on the freshly cleaved HOPG surface in 500 nm × 500 nm (above), cross section of the STM image from a to b (below). (B) STM images of CPMVA film adsorbed on the precathodized surface in 500 nm × 500 nm (above), cross section of the STM image from c to d (below). (C) Unfiltered STM image of CPMVA film adsorbed on the precathodized surface in 36 nm × 36 nm; the Fourier spectrum of raw data is shown as the inset. (D) High-resolution STM image of the bare precathodized HOPG surface.

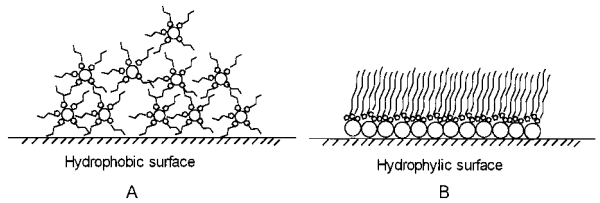

Figure 4. Proposed structural illustration of CPMVA film on the freshly cleaved HOPG electrode surface (A) and on the precathodized HOPG electrode surface (B). ○ represents $AsMo_{11}VO_{40}^{4-}$ anion, and ⬠〰 represents cetyl pyridinum cation.

Figure 3B shows a typical macroscale STM image of the CPMVA film adsorbed on the precathodized HOPG surface. Different from the CPMVA film on the freshly cleaved HOPG surface, no any domain structures or aggregates can be observed even at the edge of step (surface height difference of CPMVA film is only about several angstroms estimated from the cross section), which strongly suggests that the CPMVA film is homogeneously adsorbed on the precathodized HOPG surface without forming partial multilayers or aggregates. Typical and raw high-resolution images of the CPMVA film adsorbed on precathodized HOPG surface are shown in Figure 3C. The inset shows the two-dimensional Fourier spectrum of the image, in which the sixfold symmetry spots are seen. CPMVA molecules clearly exhibit a hexagonal-lattice

Table 1. XPS Spectra of Different Elements for CPMVA Film on Various HOPG Surfaces

	N_{1s} % (401.2 eV)	Mo_{3d} % ($Mo_{3d5/2}$ = 235.8 eV, $Mo_{3d3/2}$ = 232.6 eV)	V_{2p} % (517.7 eV)
CPMVA film on the freshly cleaved HOPG surfaces	3.9	10.9	1.0
CPMVA film on the precathodized HOPG surfaces	4.0	11.2	1.0

ordered array. Compared with the high-resolution STM image of the bare precathodized HOPG surface (Figure 3D), the distance between adjacent molecules in the STM image of CPMVA films is larger. The nearest-neighbor distance in all molecular directions is between 10 and 11 Å. It is consistent with the X-ray crystallographic results of $AsMo_{11}VO_{40}^{4-}$ anion,[16] which is the negatively charged part of CPMVA. After 30-day time aging or immersion into aqueous solution, the CPMVA film remains uniform and less aggregation has occurred. It demonstrates that the CPMVA film adsorbed on the precathodized HOPG electrode surface is quite stable.

Figure 4 presents the possible schematic structural illustration of CPMVA molecules on bare or precathodized HOPG electrode. When CPMVA molecules are adsorbed on a freshly cleaved HOPG in organic solvents, because the freshly cleaved HOPG surface and organic solvents are all hydrophobic, CPMVA molecules aggregate to remain stable with hydrophilic $AsMo_{11}VO_{40}^{4-}$ anions inside and hydrophobic alkyl chains outside (as shown in Figure 4A).[17] So CPMVA molecules tend to form self-aggregated clusters on a poorly hydrophilic surface, as shown in the STM image of Figure 3A.

After the HOPG is precathodized, the hydrophobic electrode surface is changed to be hydrophilic and some functional groups, such as hydroxyl, carbonyl, ether, and phenolic, are introduced.[18] When CPMVA molecules are adsorbed on the precathodized HOPG electrode surface in organic solvents, the $AsMo_{11}VO_{40}^{4-}$ anion of CPMVA adsorbed on the hydrophilic electrode surface and the alkyl chains of CPMVA are faced with the organic solvents in order to attain the stable state (as shown in Figure 4B).[19] Moreover, the strong interaction between Mo(VI) of the $AsMo_{11}VO_{40}^{4-}$ anion and the functional groups of precathodized HOPG surface enhances the structure stability of CPMVA film (see later section 4a). CPMVA molecules tend to form a self-organized monolayer on a precathodized HOPG surface, as shown in the STM image of Figure 3C. The $AsMo_{11}VO_{40}^{4-}$ anion of CPMVA, instead of the hydrocarbon of CPMVA, can be observed in the STM image. This is because the tip of the microscope is in the hydrocarbon domain of the CPMVA film, similar to the STM image of the self-assembly thiol on the Au electrode.[20] The average area of each pyridine ring is ~21 Å^2 (by Arvial et al.[21]), while the surface area of each $AsMo_{11}VO_{40}^{4-}$ anion is much larger than 100 Å^2 as a global molecule (with 5.3 Å the radius of an $AsMo_{11}VO_{40}^{4-}$ anion[15]). So the $AsMo_{11}VO_{40}^{4-}$ anion surface has plenty space for adsorbing four cetyl pyridinum cations to maintain the electroneutrality of the CPMVA film. On the other hand, it shows that the cetyl pyridinum cation cannot form closest-packing on the electrode surface.

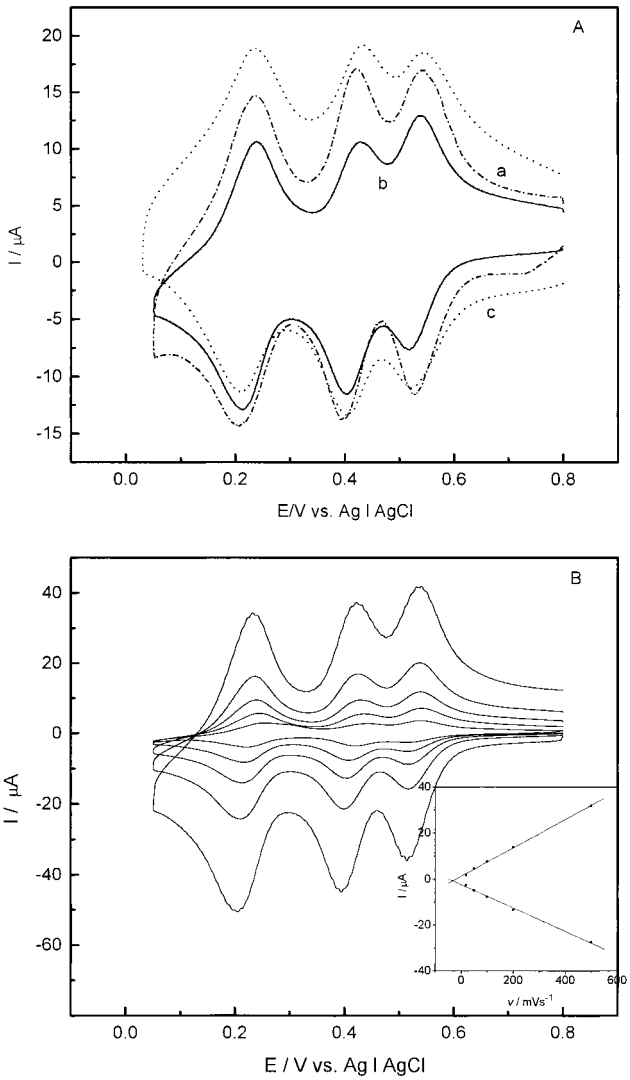

Figure 5. (A) Cyclic voltammograms of CPMVA film on the freshly cleaved HOPG electrode (curve a), on the precathodized HOPG electrode (curve b), and $H_4AsMo_{11}VO_{40}$ film on the precathodized HOPG electrode (curve c) in 0.5 M H_2SO_4. Scan rate: 100 mV s^{-1}. (B) Cyclic voltammograms of CPMVA film on the precathodized HOPG electrode in 0.5 M H_2SO_4 at different scan rates. The inset shows variation of the cathodic and anodic peak currents ($E_{1/2}$ = 0.225 V) with scan rates.

4. Electrochemical Behavior of the CPMVA Film. *4a. Electrochemical Behavior of the CPMVA Film in Aqueous Solution.* Figure 5A presents the voltammetric behavior of the CPMVA film on a freshly cleaved HOPG electrode (curve a), the CPMVA film on the precathodized HOPG electrode (curve b), and the $H_4AsMo_{11}VO_{40}$ film on the precathodized HOPG electrode (curve c). It must be emphasized that although both precathodization and preanodization make the HOPG surface hydrophilic,

(16) (a) Keggin, J. F. *Nature* **1934**, *144*, 75. (b) Evans, H. T. *Inorg. Chem.* **1966**, *5*, 967. (c) Izumi, Y.; Hasebe, R.; Urabe, K. *J. Catal.* **1983**, *94*, 402. (d) Highfield, J. G.; Moffat, J. B. *J. Catal.* **1984**, *88*, 177.

(17) Zhang, J.; Chi, Q.; Dong, S.; Wang, E. *Bioelectrochem. Bioenerg.* **1996**, *39*, 267.

(18) (a) Evans, J. F.; Kuwana, T. *Anal. Chem.* **1977**, *49*, 1635. (b).Horber, J. K. H.; Lang, C. A.; Hansch, J. W.; Heckl, W. M.; Mohwald, H. *Chem. Phys. Lett.* **1988**, *145*, 151. (c) Rice, R. J.; McCreery, R. L. *Anal. Chem.* **1989**, *61*, 1637. (d) McCreery, R. L. In *Electroanalytical Chemistry*; Bard, A. J., Ed.; Marcel Dekker: New York, 1990; Vol. 17. (e) Ilangovan, G.; Pillai, K. C. *Langmuir* **1997**, *13*, 566. (f) Dong, S.; Wang, B. *Electrochim. Acta* **1992**, *37*, 11.

(19) (a) Fujiwara, I.; Ohnishi, M.; Seto, J. *Langmuir* **1992**, *8*, 2219. (b) Yeo, Y. H.; McGonigal, Yackoboski, K.; Guo, C. X.; Thomson, D. J. *J. Phys. Chem.* **1992**, *96*, 6110. (C) Maoz, R.; Sagiv, J. *J. Colloid Interface Sci.* **1984**, *100*, 465.

(20) Finklea, H. O. In *Electroanalytical Chemistry*; Bard, A. J., Rubinstein, I., Eds.; Marcel Dekker: New York, 1996; Vol. 19.

(21) Gomez, M. M.; Garcia, M. P.; Fabian, J. S.; Vazquez, L.; Salvarezza, R. C.; Arvia, A. J. *Langmuir* **1997**, *13*, 1317.

actually adsorption of CPMVA is totally absent on the preanodized electrode. Similar results have reported on Mo(VI) adsorbed on glassy carbon surface by our group and Pillai's group.[18e,f] The main functional groups introduced by preanodization are carboxylic, carbonyl, quinone, etc., while the main functional groups introduced by precathodization are alcohol, phenol, ether, etc.[18] The specific interaction between the Mo(VI) of the CPMVA molecule and the alcohol group of the precathodized surfaces may be advantageous for the adsorption of the CPMVA film.[18e,f] The detailed adsorption mechanism of the CPMVA film on various properties of the substrate needs further study.

As shown in Figure 5, the cyclic voltammograms of the CPMVA film (curves a and b) display three redox couples with the $E_{1/2}$ of 0.527, 0.416, and 0.225 V, and ΔE_p is less than 30 mV, corresponding to three two-electron processes, which present the same features shown for the $H_4AsMo_{11}VO_{40}$ film on the precathodized HOPG electrode in acidic aqueous solution (curve c). This shows that the cetyl pyridinum cations of the CPMVA molecule do not change the electrochemical properties of $AsMo_{11}VO_{40}^{4-}$. Otherwise, the background current of curve c is much larger than that of curves a and b, because of the inserting alkyl chains of CPMVA between the electrode and the electrolyte ions leading to a substantial reduction of interfacial capacitance, which has been shown by all the studies on the question of SAM.[20]

The CPMVA film shows the characteristics of reversible surface redox behavior on both freshly cleaved and precathodized HOPG surfaces. Figure 5B represents cyclic voltammograms of the CPMVA film on precathodized HOPG electrode in 0.5 M H_2SO_4 at various scan rates v. Typically, a plot of cathodic or anodic peak current as a function of v is linear up to 500 mV s^{-1} with a zero intercept. Their peak potentials do not vary with v.

The dependence of CPMVA adsorption on electrode pretreatment is better illustrated by using the surface coverage. An estimate of the surface coverage of CPMVA can be calculated according to the following equation as

$$\Gamma_0 = Q/nFA$$

where Γ_0, Q, and A represent the surface coverage of the redox species (mol cm^{-2}), quantity of electric charge (C), and electrode area (cm^2) measured with $Fe(CN)_6^{3-/4-}$. The CPMVA film on the precathodized electrode gives a surface coverage of 1.9×10^{-10} mol cm^{-2}. It is clear that the adsorbed film corresponds to a close-packed monolayer because a theoretical coverage of the close-packed monolayer is 1.8×10^{-10} mol cm^{-2} assuming 5.3 Å for the radius of the $AsMo_{11}VO_{40}^{4-}$ anion.[15]

However, the CPMVA film on a freshly cleaved HOPG electrode shows similar voltammetric behavior, giving a surface coverage of 2.8×10^{-10} mol cm^{-2}. This value is obviously larger than that of the CPMVA film on the precathodized HOPG electrode. It is also demonstrated that there must be multilayers or aggregates of CPMVA on freshly cleaved HOPG surface.

After the potential was cycled between 0.70 and 0.0 V at 100 mV s^{-1} in 0.5 M H_2SO_4 for 1 h, a decrease in the cathodic currents of curves a and b is less than 10%, which indicates that the CPMVA film on HOPG electrodes has a good stability in acid solution.

The electrochemical properties of the CPMVA film on different carbon substrates are also studied for comparison (the cyclic voltammograms of CPMVA film on glassy carbon electrode are shown in the Supporting Information). It is noticed that the CPMVA film on glassy carbon electrode has similar voltammetric behavior comparing to that on HOPG electrodes, which shows the CPMVA film can be successfully fabricated and maintains its electrochemical activity on various kinds of carbon surfaces.

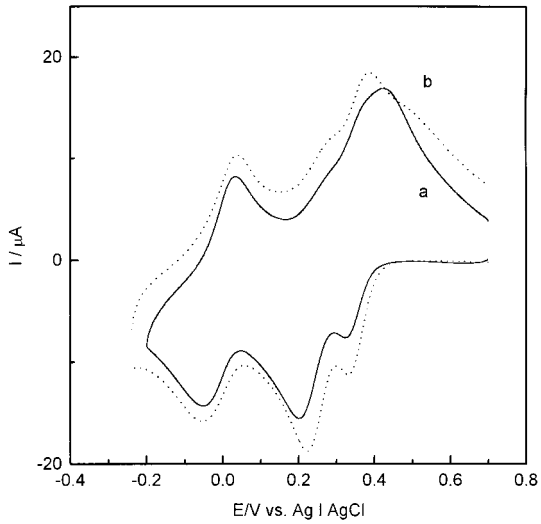

Figure 6. Cyclic voltammograms of the CPMVA-modified HOPG electrode in AC + 0.1 M $LiClO_4$ solution (solid line is CPMVA film on the precathodized HOPG electrode and dotted line is CPMVA film on the freshly cleaved HOPG electrode). Scan rate: 100 mV s^{-1}.

4b. Electrochemical Behavior of the CPMVA Film in Organic Solvent. The CPMVA film adsorbed on HOPG electrodes is also examined in organic solvent. Figure 6 presents the voltammetric behavior of the CPMVA film on a freshly cleaved HOPG electrode (···) and on the precathodized HOPG electrode (—) in acetone solution. Comparing with the solution containing CPMVA (shown in Figure 1a), the cyclic voltammograms of the CPMVA-modified HOPG electrode show less peak-to-peak separation. This is because the distance between CPMVA molecules in acetone and electrode surface is far and the rate of electron transfer of electroactive CPMVA molecules in organic solvent is slow; on the contrary, the distance between adsorbed CPMVA molecules and electrode surface is very close and the electrochemical response is fast.

Moreover, these cyclic voltammograms do not change upon potential cycling or when the electrodes are left in the electrolyte solution for a prolonged period (>10 days), which indicates the strength and nature of the irreversible adsorption of the redox components. These are all favorable for exerting the electrocatalytical function of the polyoxometalate in organic solvent.

4c. Permeation Test. The packing degree of the CPMVA film on the precathodized HOPG electrode is assessed by investigating its blocking effect on the redox electrochemistry of water-soluble $Fe(CN)_6^{3-/4-}$ ions. Figure 7 presents the well-known reversible voltammetric behavior of $Fe(CN)_6^{3-/4-}$ on a bare HOPG electrode (···), a $H_4AsMo_{11}VO_{40}$ film modified precathodized HOPG electrode (—·—), and a CPMVA film modified precathodized HOPG electrode (—). The modification of $H_4AsMo_{11}VO_{40}$ film and CPMVA film leads to a decrease of the peak currents of $Fe(CN)_6^{3-/4-}$, which indicates that the two films can hinder the redox reaction of $Fe(CN)_6^{3-/4-}$ for some extent. Because $AsMo_{11}VO_{40}^{4-}$ anions of CPMVA film expel $Fe(CN)_6^{3-/4-}$ anion transfer and the alkyl chains of CPMVA film limit access of the $Fe(CN)_6^{3-/4-}$ anion to the electrode surface, the peak current of $Fe(CN)_6^{3-/4-}$ is the smallest one on the CPMVA film modified precathodized HOPG electrode.

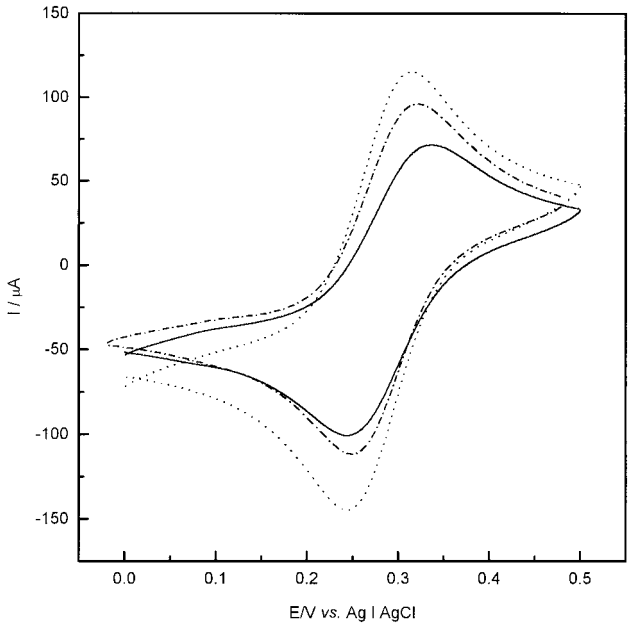

Figure 7. Cyclic voltammograms of 5 mM $Fe(CN)_6^{3-/4-}$ on a bare HOPG electrode (···), $H_4AsMo_{11}VO_{40}$ film modified precathodized HOPG electrode (—·—) and CPMVA film modified precathodized HOPG electrode (—). Scan rate: 100 mV s^{-1}.

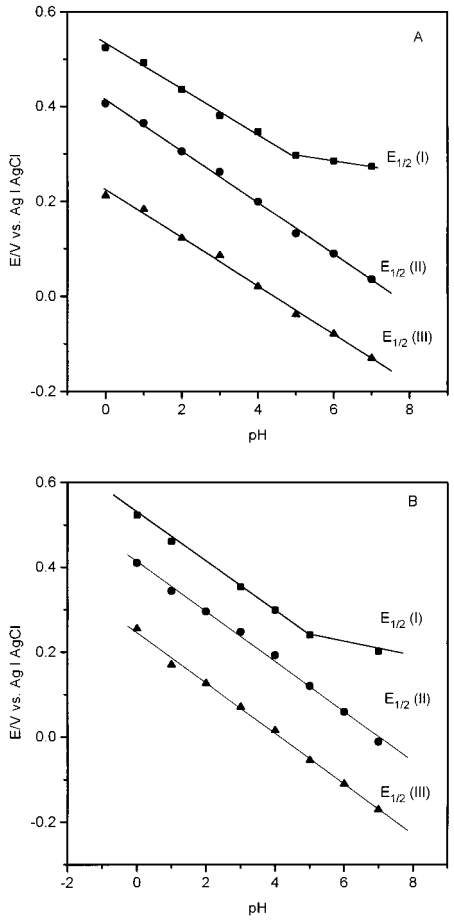

Figure 8. Relationship between peak potentials and pH for CPMVA film on the precathodized (A) and the freshly cleaved (B) HOPG electrode.

However, the peak current of $Fe(CN)_6^{3-/4-}$ is still fairly large, indicating that the $Fe(CN)_6^{3-/4-}$ ion can penetrate the alkyl chains of CPMVA film and exchange electrons with the underlying HOPG electrode. The experiment indicates that the alkyl chains of CPMVA film have a relatively loose packing structure, which provides the free space for the ion penetration. The result is consistent with the discussion in the section on characterization.

4d. pH Effect. The pH of the solution has a great effect on the electrochemical behavior of the CPMVA film modified electrode. Figure 8 shows the dependence of $E_{1/2}$ of the CPMVA film modified precathodized HOPG electrode (A) and freshly cleaved HOPG electrode (B) on the pH of the solution. For the CPMVA film both on freshly cleaved electrode and on precathodized (as shown in Figure 5a), in the range of pH ≤7.0, as the pH increases, the shapes of redox peaks remain unchanged, and the $E_{1/2}$ values of all three redox couples shift negatively. Plots of $E_{1/2}$ for the first redox waves vs pH for the film have two linear regions: in the pH range of 1−5, the average slope is −60 mV/pH, close to the theoretical value −60 mV/pH for $2e^-/2H^+$, confirming the addition of two H^+ to the two-electron reduction form of $AsMo_{11}VO_{40}^{4-}$ when the pH ≤5.0; in the pH range of 5−7, the $E_{1/2}$ stays almost unchanged, which shows that no protonation occurs in this pH range. Plots of $E_{1/2}$ for the second and third redox waves vs pH for the film demonstrate the addition of two H^+ to the four-electron and six-electron reduction forms of $AsMo_{11}VO_{40}^{4-}$ when the pH ≤7.0. The above results allow us to describe the three overall redox processes of the CPMVA film on both HOPG electrodes in aqueous solution of pH ≤7.0 as follows:

pH ≤5.0

I. $AsMo_{11}VO_{40}^{4-} + 2e^- + 2H^+ \rightleftharpoons H_2AsMo_{11}VO_4^{4-}$

II. $H_2AsMo_{11}VO_{40}^{4-} + 2e^- + 2H^+ \rightleftharpoons H_4AsMo_{11}VO_{40}^{4-}$

III. $H_4AsMo_{11}VO_{40}^{4-} + 2e^- + 2H^+ \rightleftharpoons H_6AsMo_{11}VO_{40}^{4-}$

pH > 5.0

I. $AsMo_{11}VO_{40}^{4-} + 2e^- \rightleftharpoons AsMo_{11}VO_{40}^{6-}$

II. $AsMo_{11}VO_{40}^{6-} + 2e^- + 2H^+ \rightleftharpoons H_2AsMo_{11}VO_{40}^{6-}$

III. $H_2AsMo_{11}VO_{40}^{6-} + 2e^- + 2H^+ \rightleftharpoons H_4AsMo_{11}VO_{40}^{6-}$

The above results indicate that the pH dependence of CPMVA film is much smaller than that of $H_4AsMo_{11}VO_{40}$ in acidic aqueous solution; the latter is stable at pH <4.0 and decomposes when pH >4.0. This suggests that the electrostatic attraction between cetyl pyridinum cation and $AsMo_{11}VO_{40}^{4-}$ can improve the stability of the CPMVA film, which is very useful in the preparation of modified electrode and the catalytic reaction.

5. Electrocatalytical Reduction of BrO_3^- with the CPMVA Film. The reduction of BrO_3^- is totally irreversible on bare HOPG electrode in acidic aqueous solution and does not take place prior to the evolution of hydrogen. However, the HOPG electrode modified by CPMVA film can catalyze the reduction of BrO_3^-. The electrocatalytical reduction of BrO_3^- with the CPMVA film on the precathodized HOPG electrode was recorded in Figure 9A.

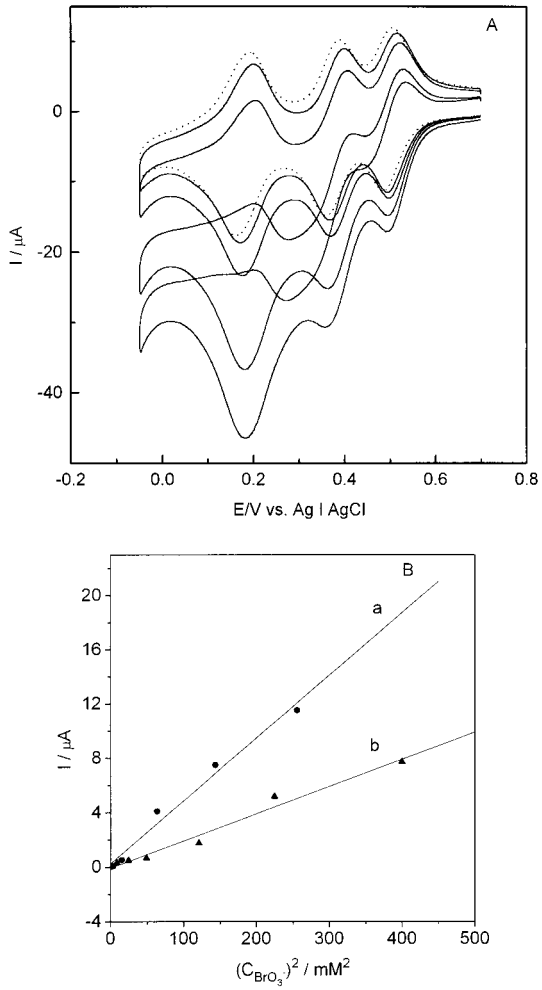

Figure 9. Electrocatalytic reduction of BrO_3^- with the CPMVA film in 2 M H_2SO_4 solution: (A) CPMVA film on the precathodized HOPG electrode, $C_{BrO_3^-}$: 0, 7, 11, 15, 20 mM (from top to bottom); (B) dependence of the catalytic current (I_{cat}) on the square of the concentration of BrO_3^- $(C_{BrO_3^-})^2$ (●, freshly cleaved HOPG electrode; ▲, precathodized HOPG electrode).

The electrocatalysis occurs at the second wave of the CPMVA film with the addition of BrO_3^-. The cathodic current of the second wave enhances, while the corresponding oxidation peak decreases, which indicates that the BrO_3^- anion is reduced by the four-electron reduction form of $AsMo_{11}VO_{40}^{4-}$ anion. A similar phenomenon has been observed for $PMo_{12}O_{40}^{4-}$ immobilized into polypyrrole film[8c] and at the WO_3 film.[22] Figure 9B shows that the catalytic current is proportional to the square of the BrO_3^- concentration during the electrocatalytic reduction with CPMVA film on both freshly cleaved HOPG electrode (curve a) and precathodized HOPG electrode (curve b). The above results demonstrate that the catalytic process is regarded as an EC catalytic mechanism. For the CPMVA film on freshly cleaved or precathodized HOPG electrode, the catalytic process can be expressed as

$$H_2AsMo_{11}VO_{40}^{5-} + 2e^- + 2H^+ \rightleftharpoons H_4AsMo_{11}VO_{40}^{5-}$$

$$H_4AsMo_{11}VO_{40}^{5-} + BrO_3^- + 4H^+ \rightleftharpoons H_2AsMo_{11}VO_{40}^{5-} + Br^- + 3H_2O$$

By comparing curve a with curve b, it is found that the catalytic currents of the CPMVA film on freshly cleaved HOPG electrode are larger than those on precathodized HOPG electrode.

Conclusion

A new polyoxometalate-based organic/inorganic film (CPMVA film) on the HOPG surface is formed by electrochemical methods. XPS results indicate that the CPMVA film is successfully immobilized on the HOPG surface and the molecular composition of CPMVA is not changed. STM studies demonstrate that the dispersion of CPMVA film strongly depends on the surface properties of the substrate: CPMVA molecules tend to form self-aggregated clusters on the freshly cleaved HOPG surface (a poorly hydrophilic surface), but to form a two-dimensional ordered monolayers on the precathodized HOPG surface (a hydrophilic and functionalized surface). The CPMVA films on both freshly cleaved HOPG electrode and precathodized HOPG electrode show reversible voltammetric responses and good stability either in aqueous solution or in organic solvent. The CPMVA and $H_4AsMo_{11}VO_{40}$ films have similar voltammetric behavior in 0.5 M H_2SO_4; moreover, the pH dependence of the redox process of CPMVA film is smaller than that of $H_4AsMo_{11}VO_{40}$ in acidic aqueous solution, which suggests that the cetyl pyridinum cation does not affect the electrochemical properties while improving the stability of the composite film. The CPMVA films both on freshly cleaved HOPG electrode and precathodized HOPG electrode show high catalytic activity in electrocatalytical reduction of BrO_3^-. Our work indicates that the CPMVA molecule not only retains electrochemical and catalytic activity of $H_4AsMo_{11}VO_4$ but also improves its stability and may be used as a catalyst in organic solvent. Thus, one can improve the physicochemical properties of polyoxometalate through molecular level design.

In addition, the new polyoxometalate-based amphiphilic material can be formed to high-degree ordered multilayers on various substrates by the LB technique.[11] We emphasize the possibility to create molecular devices having particular magnetic, catalytic, electrocatalytic, electrochromic, and photochromic properties, only through appropriate choice of polyoxometalate and lipid molecules. We are actively engaged in experiments to design these new materials.[23]

Acknowledgment. This work has been supported by the National Natural Science Foundation of China.

Supporting Information Available: Electrocatalytical reduction of BrO_3^- with $AsMo_{11}VO_{40}^{4-}$ anion inside an homogeneous solution and cyclic voltammograms of the CPMVA film on glassy carbon electrode (4 pages). This material is available free of charge via the Internet at http://pubs.acs.org.

LA991348E

(22) Kulesza, P. J.; Faulker, L. R. *J. Am. Chem. Soc.* **1988**, *110*, 4905.
(23) Liu, S.; Tang, Z.; Wang, E.; Dong, S. *Thin Solid Films* **1999**, *339*, 277.